J. Chem. Sci., Vol. 118, No. 1, January 2006, pp. 99–103. © Indian Academy of Sciences.

Structural, magnetic and magnetotransport properties of $La_{0.7-x}Ce_xBa_{0.3}MnO_3$ (x = 0·0–0·4)

R VENGADESH KUMARA MANGALAM and A SUNDARESAN*

Chemistry and Physics of Materials Unit, Jawaharlal Nehru Centre for Advanced Scientific Research, Jakkur PO, Bangalore 560 064
e-mail: sundaresan@jncasr.ac.in

Abstract. Structural, magnetic and magnetotransport properties of $La_{0.7-x}Ce_xBa_{0.3}MnO_3$ (x = 0–0·4) have been investigated although some unreacted secondary phases of CeO_2 were present. The rhombohedral structure (R-3c) for x = 0 transforms to orthorhombic with the space group *Imma* for x = 0·3. All samples showed ferromagnetic transition above 300 K and a negative magnetoresistance. For x > 0·1, magnetization data measured at 1 T showed a decrease at low temperatures (T < 50 K) due to antiferromagnetic coupling between Ce-local moments and Mn-moments. For x = 0·4, the resistivity showed a maximum around 200 K which corresponds to ordering temperature of cerium. Since these results are similar to that observed in the Sr-containing $La_{0.5-x}Ce_xSr_{0.5}MnO_3$ (x = 0–0·4) system, we suggest that the cerium ions are in the trivalent state and the anomalous behaviour has been attributed to a Kondo-like effect.

Keywords. X-ray diffraction; magnetization, magnetoresistance, manganites.

1. Introduction

Doped rare earth manganese oxides $R_{1-x}A_xMnO_3$ (R = trivalent rare earth: A = divalent alkaline earth) with perovskite structure have been the subject of intensive research in condensed matter because they exhibit very interesting properties such as colossal magnetoresistance (CMR), charge, orbital and spin ordering.[1–3] The origin of the CMR effect in these doped manganites may be understood on the basis of double exchange interaction between Mn^{3+} and Mn^{4+} ions and charge-spin-lattice coupling.[4–6] A large number of materials with various rare earth elements including those containing 4f local moments have been investigated. We were interested in studying the effect of substitution of cerium at the A-site because of the fact that cerium can exist in tri-, tetra and mixed-valence states and thereby influence the structure and properties. We have found that Ce ions exist in a trivalent state in Sr-containing manganites.[7,8] On the other hand, it has been reported that in calcium-containing $Ca_{0.9}Ce_{0.1}MnO_3$, the Ce ions are in the tetravalent state.[9] Interestingly, we found that substitution of cerium leads to a Kondo-like effect in a large band width material (W) $Pr_{0.1}Ce_{0.4}Sr_{0.5}MnO_3$.[7] In this system the Mn-moments undergo a ferromagnetic ordering at 250 K due to double exchange (DE) interactions, and Ce moments order antiferromagnetically with respect to Mn moments below $T \sim 120$ K. The electrical resistivity increases anomalously with decrease in temperature, particularly below the Curie temperature T_C, exhibiting a resistivity maximum at 120 K (T_{max}), which corresponds to the ordering of Ce moments, and a minimum at 15 K (T_{min}). The anomalous temperature dependence of resistivity $r(T)$ is in contrast to the expected metallic behaviour below T_C due to DE interactions. Similar results were reported for $La_{0.1}Ce_{0.4}Sr_{0.5}MnO_3$ with the ferromagnetic ordering of Mn-moments at $T_C \sim 280$ K and Ce ordering below $T \sim 130$ K.[8] In these systems with larger W, since there is no charge ordering of manganese ions and the Mn-sublattice remains ferromagnetic down to 1·8 K, the resistivity anomaly has been attributed to Kondo-like scattering of Mn:e_g conduction electrons by the localized Ce:4f moments. The decrease of resistivity below T_{max} or cerium-ordering temperature is due to reduced spin-dependent scattering.

In this report, we present the results on the effect of cerium substitution in Ba-containing $La_{0.7-x}Ce_xBa_{0.3}MnO_3$. It is well known that the perovskite

Dedicated to Prof J Gopalakrishnan on his 62nd birthday
*For correspondence

$BaCeO_3$ is a thermodynamically stable phase. For this reason we chose a ferromagnetic composition with low concentration of barium, i.e. a substitution level of 30%. The results of magnetic and magneto-transport properties are very much similar to that observed in cerium-substituted Sr-containing compounds as discussed above.

2. Experimental

Polycrystalline samples of $La_{0.7-x}Ce_xBa_{0.3}MnO_3$ (x = 0–0·4) were prepared by calcinations of stoichiometric mixtures of La_2O_3, CeO_2, $BaCO_3$, Mn_2O_3 at 1100°C and sintering at 1500°C. Phase purity and structural analysis were carried out with powder X-ray diffraction (XRD) data by the Rietveld analysis method using the program Fullprof.[10] Morphology and grain size were analysed by scanning electron microscope. Magnetization measurements were carried out with a vibrating sample magnetometer in physical property measuring system (PPMS, Quantum Design, USA). Magnetoresistance measurements were made by a standard four-probe method with PPMS by an applied field of 7 T.

3. Results and discussion

For x = 0, the structure is consistent with rhombohedral system (space group R-3c) as already reported.[11] The structure remains rhombohedral up to x = 0·2 and for x = 0·3 and 0·4, it could be described by an orthorhombic phase with the space group *Imma* as expected from the analysis of octahedral distortion as a function of A-site cations.[12] In all the cerium-substituted samples, a secondary phase of unreacted CeO_2 was present. In addition, in the case of x = 0·4, a small amount of $BaCeO_3$ phase could be seen as expected. These phases were included in the refinement as secondary phases. The observed, calculated and difference XRD patterns, for x = 0·0 and 0·3, obtained from the Rietveld refinement are shown in figure 1. Vertical tick marks are symmetry allowed reflections. The first row belongs to the main phase and the second one is due to the CeO_2 impurity phase. The structural parameters for x = 0·1 and 0·3 are given in table 1.

Temperature dependence of magnetic susceptibility (c) measured at 0·01 T by a field-cooling process is shown in figure 2. From this figure we can see that all the samples show ferromagnetic transition above 300 K. For x = 0·1, the transition temperature has increased to ~340 K from ~320 K for x = 0. Further increase of x leads to decrease of T_C which is consistent with the fact that the bigger La^{3+} ions are substituted by smaller Ce^{3+} ions which results in the reduction of one electron band width W. For x = 0·1, the temperature dependence of susceptibility shows a tendency to decrease below ~200 K. In fact, a clear decrease of susceptibility at low temperatures (<50 K) can be seen from the susceptibility data measured at 1 T as shown in figure 3. This indicates an antiferromagnetic coupling between the ferromagnetic Mn-moments and Ce-moment as observed in the system $La_{0.1}Ce_{0.4}Sr_{0.5}MnO_3$. Above the ferromagnetic transition temperature, the susceptibility of all the samples follows the Curie–Weiss behaviour.

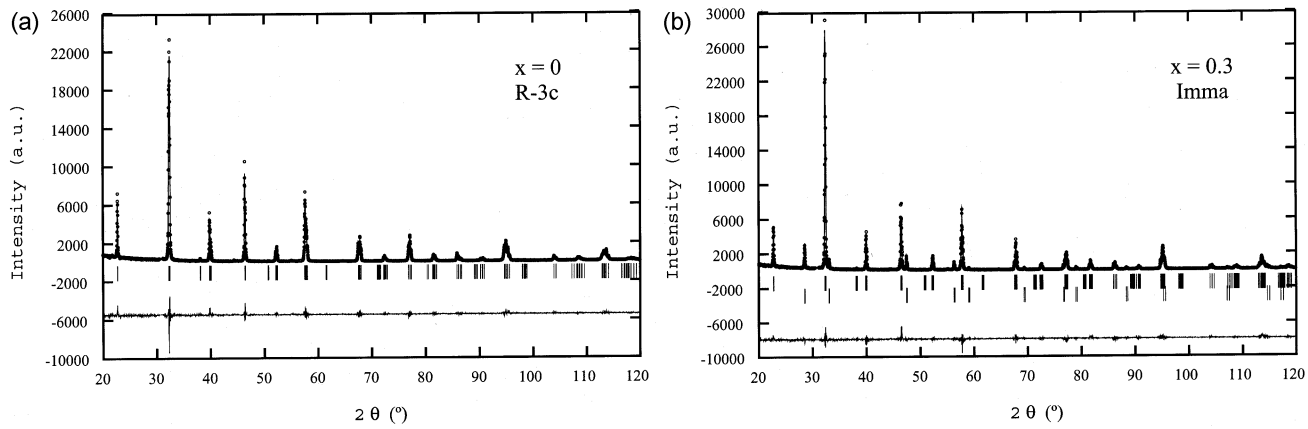

Figure 1. Observed, calculated and difference X-ray diffraction patterns of $La_{0.7-x}Ce_xBa_{0.3}MnO_3$ (x = 0 (**a**) and x = 0·3 (**b**)). Vertical tick marks are symmetry-allowed reflections and the second row corresponds to the CeO_2 secondary phase.

The effective magnetic moment derived from the Curie–Weiss fit is larger (5·18–5·40 m_B) than the expected (~4·59 m_B) for 30% hole-doping. The observed higher values of magnetic moment may indicate the presence of short-range ferromagnetic interactions above the Curie temperature. Values of q_P, the paramagnetic intercept obtained from the fit are consistent with the observed variation of T_C with x as shown in table 2.

Temperature dependence of resistivity $r(T)$ measured under zero applied field is shown in figure 4. The $r(T)$ behaviour is similar to that observed in $La_{0·5–x}Ce_xSr_{0·5}MnO_3$.[8] Just above 300 K, all samples show a peak which corresponds to ferromagnetic transition temperature that is consistent with the susceptibility measurements as discussed above. The increase of resistivity with decrease of temperature above T_C is believed to be due to large ionic size

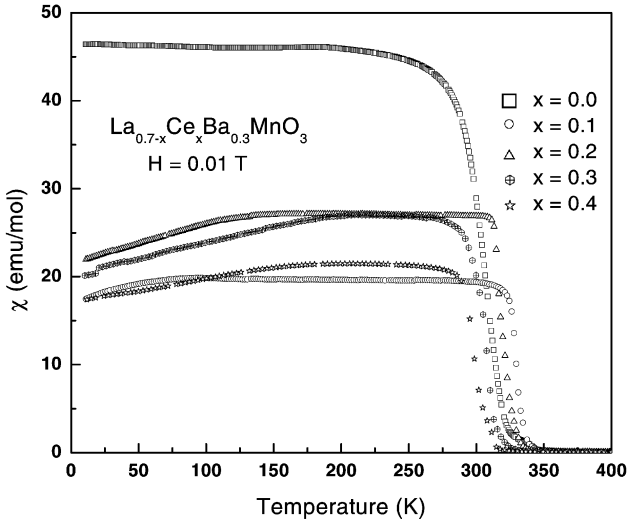

Figure 2. Variation in magnetic susceptibility, measured at 0·01 T in field-cooled process, for various x in $La_{0·7–x}Ce_xBa_{0·3}MnO_3$ as a function of temperature.

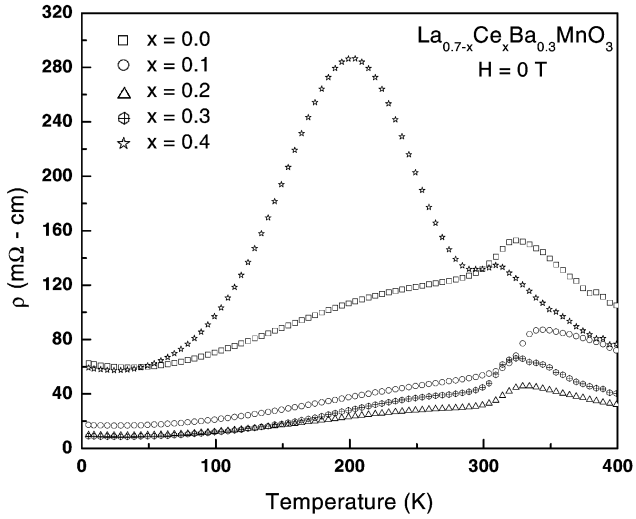

Figure 4. Temperature dependence of resistivity under zero applied field for various x in $La_{0·7–x}Ce_xBa_{0·3}MnO_3$. The peak around 200 K in $x = 0·4$ indicates the ordering temperature of cerium moments.

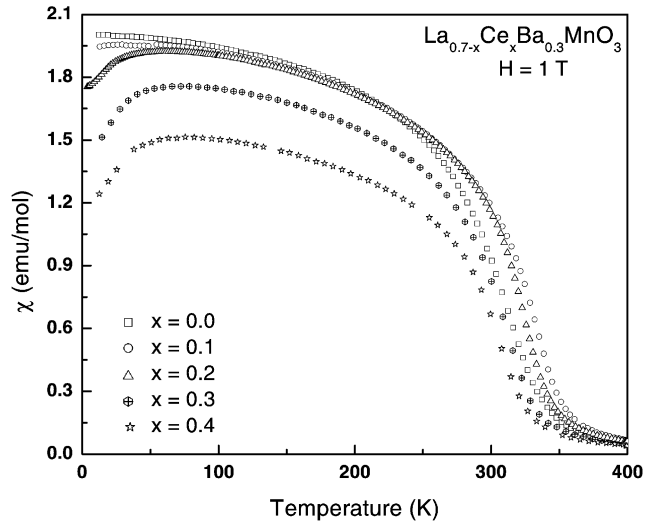

Figure 3. Variation in magnetic susceptibility, measured at 1·0 T in field-cooled process, for various x in $La_{0·7–x}Ce_xBa_{0·3}MnO_3$ as a function of temperature.

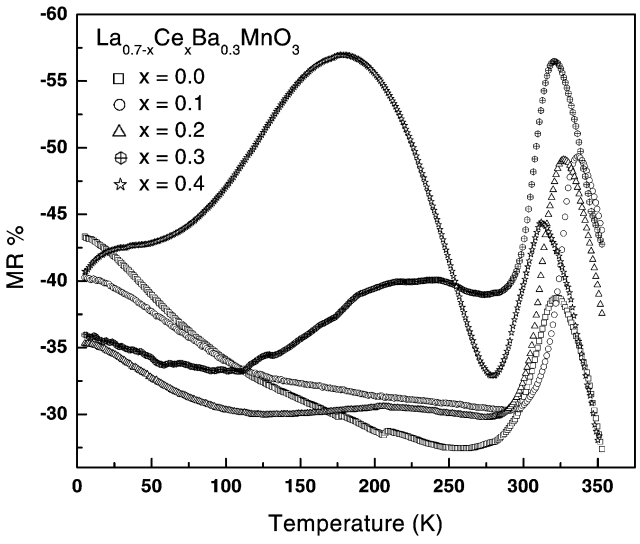

Figure 5. Temperature dependence of magnetoresistance, MR = $[r(7\ T)–r(0\ T)]/r(0\ T)$, for various x in $La_{0·7–x}Ce_xBa_{0·3}MnO_3$. The MR around 200 K in $x = 0·4$ arises due to the Ce:4*f* spin disordered scattering.

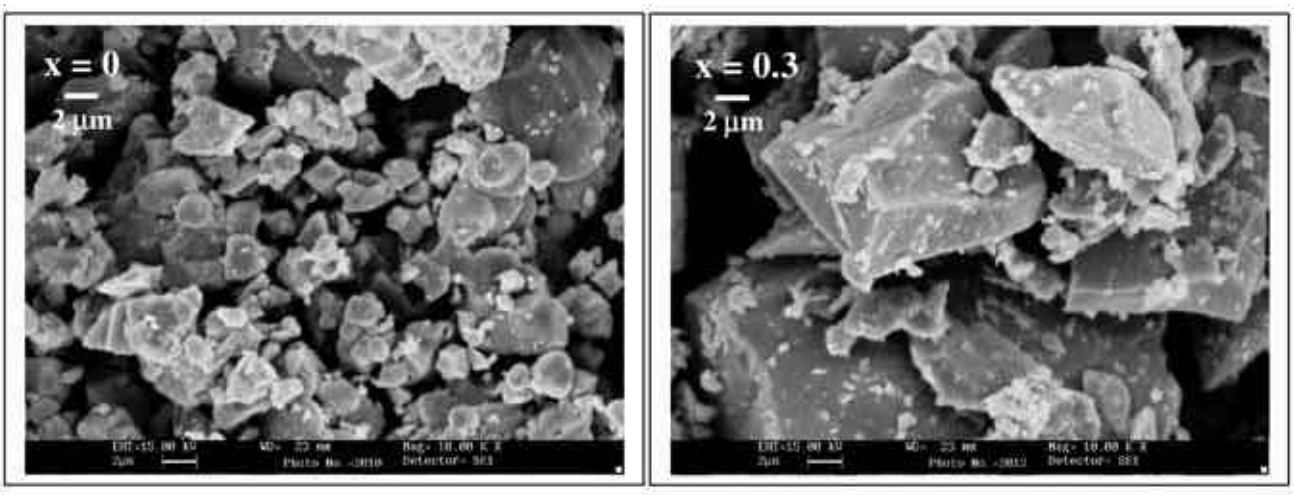

Figure 6. Scanning electron micrograph of $x = 0{\cdot}0$ and $0{\cdot}3$ in $La_{0.7-x}Ce_xBa_{0.3}MnO_3$ clearly showing that the grain size of Ce-containing sample ($x = 0{\cdot}3$) is larger than the one without cerium.

Table 1. Structural parameters of $La_{0.7-x}Ce_xBa_{0.3}MnO_3$ ($x = 0{\cdot}0$ and $0{\cdot}3$).

Parameter	$x = 0{\cdot}0$	$x = 0{\cdot}3$
Space group	*R*-3*c*	*Imma*
a (Å)	5·5470(1)	5·5221(1)
b (Å)	–	7·8044(2)
c (Å)	13·5001(3)	5·5443 (1)
V (Å^3)	359·75(1)	238·94(1)
La/Ce/Ba: *x*, *y*, *z*	0, 0, ¼	0, ¼, –0·000(1)
B (Å^2)	0·17(1)	0·16(2)
Mn: *x*, *y*, *z*	0, 0, 0	0, 0, ½
B (Å^2)	0·01(3)	0·06(4)
O(1): *x*, *y*, *z*	0·460(1), 0, ¼	½, ¼, 0·041(5)
O(2): *x*, *y*, *z*	–	½, ¼, 0·41(5)
c^2	3·83	5·54
Bragg *R* (%)	3·81	6·30

Table 2. Variation of T_C, q_P and particle size with x in $La_{0.7-x}Ce_xBa_{0.3}MnO_3$.

x	0·0	0·1	0·2	0·3	0·4
T_C (K)	327	340	330	319	312
q_P (K)	324	335	328	317	309
Particle size (*m*m)	0·3708	0·4595	0·4593	0·5396	0·5815

mismatch at the A-site.[13] For higher cerium concentration ($x = 0{\cdot}4$) there is a second resistivity maximum around 200 K which is related to an antiferromagnetic ordering of cerium moments with respect to Mn-moments. This peak cannot be attributed to ionic size mismatch because the size difference between La^{3+}(1·216) and Ce $^{3+}$(1·196) [14] is very small and there is evidence for an antiferromagnetic ordering as inferred from the susceptibility data measured at 1 T as shown in figure 3.

The scattering of Mn-e_g electrons by the localized Ce-4*f* moments is clear from the large negative magnetoresistance (MR = $[r(7\ T)–r(0\ T)]/r(0\ T)$) observed for $x = 0{\cdot}4$ in the vicinity of 200 K as shown in figure 5. All samples show large magnetoresistance above room temperature due to double exchange ferromagnetism. At low temperatures <10 K, the magnetoresistance for $x = 0$ may arise from electron tunneling between the grain boundaries. With increase of x up to 0·3, the MR decreases. This is due to increase in the grain size with increase in cerium concentration as suggested by our SEM analysis. Figure 6 compares the grain size for $x = 0$ and 0·3 samples and it is obvious that the latter has larger grain size. This is also clear from the particle size calculation done using Debye–Scherrer formula on XRD data, given in table 2. For $x = 0{\cdot}4$, however, the MR increases which is mainly due to Kondo-like scattering of Mn-e_g electrons by the Ce-4*f* moments as observed in $R_{0.1}Ce_{0.4}Sr_{0.5}MnO_3$ (R = La, Pr).[7,8]

4. Conclusions

In conclusion, the system $La_{0.7-x}Ce_xBa_{0.3}MnO_3$ transforms from a rhombohedral structure to orthorhombic at $x = 0{\cdot}3$. Its magnetization, resistivity and magnetoresistance are similar to that observed for $La_{0.5-x}Ce_xSr_{0.5}MnO_3$ suggesting a Kondo-like behaviour. This indicates that Ce ions are in trivalent state.

Acknowledgement

The authors would like to thank Prof C N R Rao for his encouragement and support.

References

1. Rao C N R and Raveau B 1998 *Colossal magnetoresistance, charge ordering and related properties of manganese oxides* (Singapore: World Scientific)
2. Ramirez A P 1997 *J. Phys. Cond. Matter* **9** 8171, and references therein
3. Jonker G H 1950 *Physica* (*Amsterdam*) **16** 337
4. Zener C 1951 *Phys. Rev*. **82** 403
5. Anderson P W and Hasegawa H 1955 *Phys. Rev.* **100** 675
6. de Gennes P-G 1955 *Phys. Rev.* **118** 141
7. Sundaresan A, Caignaert V, Maignan A, Raveau B and Suard E 1999 *Phys. Rev.* **B60** 533
8. Sundaresan A, Tholence J L, Maignan A, Raveau B, Suard E and Bordet P 2001 *J. Magn. Magn., Mater*. **226–230** 777
9. Zeng Z, Greenblatt M and Croft M 2001 *Phys. Rev.* **B63** 224410
10. Rodriguez-Carvajal 1993 *Physica* **B192** 55
11. Randaelli P G, Marezio M, Hwang H Y and Cheong S-W 1996 *J. Solid State Chem.* **122** 444
12. Barnabé A, Millange F, Maignan A, Hervieu M, Raveau B, Van Tendeloo G and Laffez P 1998 *Chem. Mater*. **10** 252
13. Rodriguez-Martinez L M and Attfield J P 1996 *Phys. Rev.* **B54** 622
14. Shannon R D 1976 *Acta Crystallogr*. **A32** 751